A Highly Portable, Rapidly Deployable System for Eddy Covariance Measurements of CO_2 Fluxes

D.P. Billesbach[*1], M.L. Fischer[2], M.S. Torn[3], and J.A. Berry[4]

[1] Dept. of Biological Systems Engineering, University of Nebraska, Lincoln, NE 68583-0726
[2] Environmental Energy Technologies Division, Lawrence Berkeley Laboratory, Berkeley, CA 94720
[3] Center for Isotope Geochemistry, Lawrence Berkeley Laboratory, Berkeley, CA 94720
[4] Dept. of Plant Biology, Carnegie Institution of Washington, Stanford, CA 94305

ABSTRACT

To facilitate the study of flux heterogeneity within a region, the authors have designed, built, and field-tested a highly portable, rapidly deployable, eddy covariance CO_2 flux measurement system. The system is built from off-the-shelf parts and was assembled at a minimal cost. The unique combination of features of this system allow for a very rapid deployment with a minimal number of field personnel. The system is capable of making high precision, unattended measurements of turbulent CO_2 fluxes, latent heat (LE) fluxes, sensible heat fluxes (H), and momentum transfer fluxes. In addition, many of the meteorological and ecosystem variables necessary for quality control of the fluxes and for running ecosystem models are measured.

A side-by-side field comparison of the system at a pair of established AmeriFlux sites has verified that, for single measurements, the system is capable of CO_2 flux accuracy of about ± 1.2 μmole/m^2/sec, LE flux accuracy of about ± 15 Watts/m^2, H flux accuracy of about ± 7 Watts/m^2, and momentum transfer flux accuracy of about ± 11 gm-m/sec/sec. System deployment time is between 2 and 4 hours by a single person. The system was measured to draw between 30 and 35 Watts of power and may be run from available line power, storage batteries, or solar panels.

Keywords; eddy correlation, eddy covariance, CO2 flux, carbon dioxide

[*] Corresponding author. Fax: (402)472-6338. Email: dbillesbach1@unl.edu

INTRODUCTION

A central question in the study of global climate change is the influence of land use and land use management on climate. While much research in carbon and energy balance has been done in forested ecosystems, only recently have similar studies begun in grasslands. Grassland and rangeland ecosystems dominate the Great Plains region of North America, and extend from central Canada, south to Texas and from eastern Nebraska, west to the Rocky Mountains. Within these ecosystems, land use variability and management practices create stark heterogeneity in vegetation cover, soil moisture, and other surface properties. Many of these differences can be observed over distances as short as hundreds of meters. Additionally, climatic, edaphic, and management practice variations can produce heterogeneity within similar vegetation types, again over short distances. Because the first priority of most flux networks has been to characterize "representative" ecosystems, there are few replicates within any given vegetation type or management regime. As a result, researchers using these data must assume that they are representative of all areas, and have no empirical estimate of site-to-site variability.

Currently, information about these ecosystems comes from heavily instrumented, permanent (or semi-permanent) flux tower sites. By their very nature, they can only explore the rather limited surrounding landscape. A further complication exists for taller towers (above 10 meters). The footprint seen by a flux tower under typical unstable conditions is usually about 100 times the height of the measuring instrumentation above the canopy. In these cases, footprints can extend out for several kilometers and encompass numerous, distinct flux zones. These "tall tower" systems thus sample a weighted average of several different flux regimes. To address these issues, a portable, high precision flux system is needed that can be set up and taken down quickly and easily and that can run without the expensive and limiting infrastructure usually associated with flux installations. By deploying several of these systems, simultaneously, differences in plot-level fluxes will be revealed.

Existing portable flux systems have shown the utility of this concept. One portable system is currently being used to cross calibrate carbon flux sites within the AmeriFlux program (Evans, 2000). While it makes precision flux measurements (using the eddy covariance technique) and is easily transported and set up, it requires the tower and power infrastructure of an existing flux site. An earlier system was used to examine spatial and climatic heterogeneity of fluxes from arctic ecosystems (Eugster et

al, 1997). Since the time that these systems were designed, however, new technology has become available that allows the design of more precise and robust, energy efficient flux systems.

To better understand the carbon dynamics of heterogeneous landscapes, we are developing a program of atmosphere-biosphere carbon exchange measurements in the Southern Great Plains (SGP) Cloud and Radiation Testbed (CART) of the DOE Atmospheric Radiation Measurement program. The ARM-CART encompasses an area of 140,000 km^2 in Oklahoma and southern Kansas. It is heavily instrumented with an advanced atmospheric observation program based at a Central Facility and at a distributed network of extended facilities, to improve understanding and modeling of cloud and convection processes in general circulation models.

The 160 acre (64 ha) Central Facility is located near the town of Lamont Oklahoma (36° 37'N, 97° 30'W). We have installed an eddy covariance CO_2 flux measurement system at the 60 m level of the meteorological tower operated by ARM. One of the project objectives is to test the use of this system as a practical way to estimate CO_2 fluxes from a large heterogeneous region. To explore this concept, we need to compare fluxes from the 60 m level with fluxes measured at the plot level, made within the 60 m tower footprint.

While most of the region surrounding the tower is primarily agricultural land, it consists of a number of distinct ecosystems. Northern Oklahoma, like most of the Great Plains, encompasses a wide range of land uses, including, prairie, rangeland, cropland, urban areas, petroleum production and refining facilities, and mixed industrial activities. The five main vegetation types are: C_4-dominated native prairie, C_3-dominated pastures, C_4 croplands, C_3 croplands, and deciduous hardwood riparian zones. The primary cultivated crop in the region is winter wheat, but there are a significant number of other crops (soy beans, maize, forage corps, and cotton), as well as pasture. Each of these land uses has distinctive seasonal and diurnal CO_2 flux patterns. Because of these various land use types and the extreme range of the 60 m flux tower (6 km or more), we expect that its footprint will be quite heterogeneous.

To address the issues mentioned above, we have designed, constructed, and tested a highly portable, rapidly deployable, precision CO_2 flux system. It takes advantage of a new infrared gas analyzer (IRGA) to reduce the power demand while increasing instrument precision, portability, and robustness. With this system, we can study the patterns of carbon flux among different land uses and among the

different replicates of the same land use, as well as explore the spatial flux heterogeneity within the 60 m tower's footprint. Additionally, it will measure most of the parameters necessary to run and validate ecosystem models (such as SiB2; Sellers et al. 1996) at much smaller scales than the 60 m tower can. By doing this, we hope to provide a bridge for scaling up from plot-level measurements to the 60-m tower measurements.

The eddy covariance method is the most direct technique available for turbulent flux measurements, and we therefore believe it is best suited to our application (Kaimal and Finnigan, 1994). Our portable flux system was designed to make precision eddy covariance flux measurements and to meet the following goals:

1. Portability. The system should be easily moved from site to site to address the issues of transient meteorological or ecological phenomena

2. Ease of setup. It should be possible for a crew of one or two field personnel to setup and run the system. This feature has the added benefit of reducing field operation costs.

3. Low power consumption and infrastructure requirements. The system should not depend on line power or other conveniences being available and should be capable of running unattended at the most remote and primitive sites for periods of several weeks. In addition, the system must be capable of making measurements necessary for quality control of fluxes and for modeling.

4. Low maintenance and high reliability. The system should be rugged enough to withstand frequent site changes. Also any required maintenance should be easily performed by the field crew with a minimal effort. We desire a system that will not experience significant down time.

5. High Accuracy. We want a system that will make flux measurements with precision and accuracy that are comparable to a permanent eddy covariance installations.

6. Low cost. By keeping the cost of the system to a minimum, we will be able to produce several copies for simultaneous deployments.

Following these criteria should result in an instrument system that will provide high precision measurements and require a minimum of infrastructure and maintenance.

Two main classes IRGAs are used to make CO_2/H_2O density measurements for eddy covariance fluxes. These are the open and the closed path types. In a closed path sensor system, air is drawn through a long sample tube from a point near a sonic anemometer, and directed through a closed cell where the actual density measurement is made. By contrast, an open path IRGA makes density measurements *in-situ*, near the sonic anemometer. One manifestation of the fundamental difference between these two types of IRGAs is the manner in which the flux data must be treated. The fundamental expression of eddy covariance fluxes is:

$$Flux = \overline{w}\,\overline{\rho} + \overline{w'\rho'}$$

Where w is the vertical wind speed and ρ is the density of the entity of interest. The overbar represents a mean value, and the prime indicates fluctuations about the mean. The second term is the familiar time average of the covariance between fluctuations in the density of the entity and the vertical wind speed. To a first approximation, the first term (the product of the means) should tend to zero. This is true in long-term averages because the mean vertical wind speed must eventually average to exactly zero. However, in averaging periods appropriate to flux measurements, (usually about 30 minutes) this is not strictly true. There can be a small mean vertical wind velocity due to buoyancy (or density) effects, which are ultimately caused by the turbulent transfer of water vapor and heat. This term, then is usually treated as a correction to the measured turbulent flux calculated from the second term. Webb, Pearmann, and Leuning (Webb et al, 1980) treated this in great detail, and derived the following expression for this correction

$$\overline{\mathbf{w}}\,\overline{\rho} = \overline{\rho}\left(\overline{\mathbf{w}'\rho'_{\mathrm{v}}}\,\frac{\mu}{\overline{\rho}_{\mathrm{A}}}\right) + \overline{\rho}\left(\overline{\mathbf{w}'\mathbf{T}'}\,\frac{1+\mu\sigma}{\overline{\mathbf{T}}}\right)$$

In this expression, ρ_V is the atmospheric density of water vapor, ρ_A is the density of dry air, μ is the ratio of the molecular weight of dry air to water vapor (about 1.61) and σ is the ratio of the mean density of water vapor to dry air. In general, then, there are two "correction" terms that should be applied to the eddy covariance fluxes. One is proportional to the latent heat flux, LE ($w'\rho_v'$) and one proportional to the sensible heat flux, H ($w'T'$). We note that this simplistic approach ignores several possible contributions to the net ecosystem exchange (NEE). (Lee, 1998, Paw U et al., 2000) It does, however suffice for the purposes of this study. It has been found, that through interactions with the sampling tube wall, temperature fluctuations (T') are completely damped out by as little as one meter of tubing. This, in effect, forces the second component of the Webb-Pearman correction to zero for a closed path analyzer, while both correction terms are important for the open path variety. Substituting typical values into the Webb Pearman equation reveals that the second term (or the H correction) can be up to an order of magnitude larger than the first term (the LE correction). In cases of low turbulent fluxes, and high sensible heat fluxes (large H), the correction can, in fact, be larger than the turbulent term, and even change the sign of the corrected flux. Because our system is based around an open path IRGA, it is imperative that we be able to accurately calculate both correction terms. Validation of these corrections therefore is one of the key objectives of this study. We mention here that other work being done by the first author has addressed exactly this issue and has shown that the Webb-Pearmann-Leuning correction can be accurately made using the IRGA chosen for this project.

INSTRUMENT DESCRIPTION

The design that was eventually chosen can be broken down into two major sub-systems. These will be referred to as the "fast response" system and the "slow response" system. This nomenclature describes the measurement speed of the instruments within each sub-system. In addition to these two sub-systems, there is also a flexible power system that is adaptable to most field sites, and a suite of data analysis software.

FAST RESPONSE SYSTEM

We will begin by discussing the fast response system. This system component is composed of two sensors, the sonic anemometer and the CO_2/H_2O IRGA. The anemometer chosen was the Gill-Solent WindMaster Pro, 3-dimensional sonic anemometer/thermometer. The analog input system contained in the

WindMaster Pro has 14 bits of resolution and accepts signals between +5V and –5V. The system consists of 4 fully differential analog inputs that may be re-configured (in pairs) to as many as 8 single ended inputs. A LiCor LI-7500 open path CO_2/H_2O infrared gas analyzer was chosen to make density measurements of CO_2 and water vapor. CO_2 and H_2O densities are converted to analog voltages by the LI-7500 (0-5V range, 16 bit resolution) and connected (at the signal junction box described below) to the WindMaster Pro analog inputs. By taking advantage of this, we avoid possible time shifting problems that could be caused by using different instrument clocks, not exactly synchronized. In essence, the data collection system samples the wind velocity and the densities of CO_2 and H_2O at a rate of 10 Hz as defined by the anemometer. While not recording the RS232 serial data stream from the LI-7500 effectively looses some of the ancillary data available from the IRGA, it simplifies the data collection system by only requiring a single RS232 serial data channel.

The fast response instruments are mounted at the top of a 10-foot tripod tower (Campbell Scientific Inc.). The sensors are mounted on a common horizontal bar such that their lateral separation can be adjusted from about 15 cm to more than 30 cm. To minimize flux loss and flow distortion, the IRGA is mounted about 25 cm below the anemometer volume (Kristensen et al., 1997). As recommended in the LiCor LI-7500 manual, the IRGA is tipped about 30° from vertical to facilitate drainage of condensation and rain from the windows. As received, the tripod tower allows the instruments to be mounted between about 3 and 4 meters above the ground. If higher or lower deployments are required, the central pole of the tower can be replaced with a longer or shorter piece of standard 1¼ inch galvanized steel water pipe. When the tower was properly deployed with its guy wires and foot pegs installed, it proved to be quite stable and vibration free, even in sustained winds of between 10 and 12 m/sec (the highest experienced on our deployments).

To record data from the fast response system, we use a small notebook computer. The particular model used (Toshiba Portege 3110CT) was chosen specifically for its low power consumption. The notebook computer is housed in a small, insulated plywood shelter. The shelter is passively cooled with a standard roof ventilator installed on top and 5 two-inch soffet vents installed in the bottom. The shelter has 4 one-inch floor flanges attached to its bottom. These allow mounting of legs to the shelter to elevate it

above the vegetation for improved ventilation. Field tests showed that the interior temperature never rose more than about 5 °C above ambient.

To facilitate quick set up of the system, a signal junction box was constructed. It was fabricated from a weather proof, polycarbonate box (Hoffman Engineering). Cables from both the anemometer and the LiCor IRGA were terminated in black plastic circular connectors (Amphenol Series One). Mating connectors were mounted to the junction box and all interconnections were made inside. Since the serial data stream from the anemometer conforms to the RS422 standard, an RS232 to RS422 converter (Telebyte Inc.) was also installed in the junction box. A similar box with mating connectors is mounted on the outside of the computer shelter. On the inside of the shelter, on a small plastic workbox attached to the wall, are mounted standard 9-pin RS232 connectors. These allow standard cables to be used for all signal connections.

SLOW RESPONSE SYSTEM

The slow response system contains instrumentation used to measure ancillary parameters needed to calculate accurate fluxes, validate their quality, and to quantify some of the ecosystem variables necessary for modeling. This sub system is called the slow response system because all of the recorded quantities are 30-minute averages. Quantities measured by this sub-system include, mean wind speed, wind direction, air temperature and relative humidity at two heights, barometric pressure, soil temperature, soil heat flux, total incoming solar radiation, photosynthetically active radiation (PAR), incoming and reflected radiation in long and short wavelength bands, and net solar radiation. The system is built around a Campbell Scientific Inc. CR23X data logger. Instruments attached to the data logger are listed in table 1. While this is the list of instruments attached to the current system, it can easily be modified for other applications. In fact, we plan to soon include instrumentation for soil moisture content measurements.

Like the fast response system, the slow response system is mounted on a Campbell Scientific Inc. 10 foot tripod tower. The tower was modified by adding a removable horizontal outrigger bar for mounting the radiometers. This bar is at a height of about 2.4 m and extends approximately 2 m out from the central tower.

The data logger is housed inside an environmental enclosure (Campbell Scientific Inc.) that attaches to the tower. To facilitate instrument set up, a signal junction box, similar to the fast response

junction box, is attached to the bottom of the data logger enclosure, with short lengths of PVC pipe. These also form wiring chases for the cables that run from the connectors on the bottom of the junction box to the terminal strips of the data logger. All of the slow response instruments are terminated in the same kind of connectors used with the fast response system or in thermocouple connectors. This approach realizes significant savings in setup time.

POWER SYSTEM

The system draws power from deep cycle marine/RV batteries. The entire system was measured to draw between 2.2 and 2.5 amps (depending on the laptop activity) at 13.6 volts (30 to 35 watts). This translates to a power requirement of between 50 and 60 amp-hours per day. For the field validation deployments, a single battery of 105 Amp-hour capacity was used. During that period, the battery was trickle charged with a commercial automotive battery charger using available line power. For deployments at less developed sites, a solar charging system is being developed. This system is modular in nature and its capacity can be adjusted as needed. Power is distributed to the different system components through 2-wire cables terminated in 4 pin, reversed gender plugs (Amphenol Series One) to avoid accidental sensor damage.

SOFTWARE

The data collection program is of our own design and was coded by the first author. This program, which runs under the MSDOS operating system, has proven reliable at two AmeriFlux sites for the last 3 years. Only a few modifications were needed to adapt the program to this project. The central function of the program is to read the serial data stream from the anemometer and store it in binary form on a hard disk. The program can operate at any of the baud rates available from the anemometer. In addition, the program does on-line unit conversions and keeps running statistics (means, variances, and covariances) from which on-line fluxes and correction factors are calculated.

While these on-line values are considered fairly accurate, proper re-processing of the raw data is necessary to obtain fluxes of the highest possible accuracy. The program used for this task (written by the first author) calculates and applies the optimum delay factor for each channel (Chahuneau et al., 1989) and removes mean values using a linear detrending technique (Rannik and Vesala, 1999). The program also calculates covariances, fluxes, and other relevant statistics. Finally, the program calculates correction

factors for all fluxes (Webb, Pearman, and Leuning, 1980), (Moore, 1986), (Schotanus et al., 1983). To estimate flux errors, the program calculated the worst possible covariance for each averaging period and calculated flux values from this. In theory, this number should represent only accidental correlations and thus provide an estimate of the flux noise.

DATA QUALITY CONTROL AND INSTRUMENT CALIBRATIONS

The quality control criteria applied to the CO_2 flux data before the regression fitting was performed are as follows. First, all averaging periods where the mean horizontal wind velocity was less than 2 m/sec were eliminated. Second, periods where the standard deviation of the CO_2 density from either the permanent or the portable system was greater than 1.1 μmole/m^3 (25 mg/m^3) were also eliminated. The former condition ensured that both flux systems were "looking at the same footprint", and the latter assured that both instruments were operating properly.

Before processing the temperature and relative humidity gradient data, all four sensors were removed from their radiation shields and bundled together. The bundle was then placed in an enclosed plastic tub with a circulating fan. Data was collected from this arrangement for about 30 minutes, after which a small light bulb was placed behind the circulating fan to heat the box. Data was collected for another 30 minutes and the light was then turned off. A final 30 minutes of data were collected. This data set was used to determine offsets between the individual sensors (both T and R.H.). These offsets were applied to the field data before gradients were calculated.

Before the first deployment, both the CO_2 and the H_2O channels of the LI-7500 were calibrated (on DOY 196). Prior to this, the IRGA had been calibrated on DOY 78. First, dry N_2 was introduced into the calibration hood. The IRGA read this as a mixing ratio of –5 ppmv. This represents a drift of the instrument offset. The offset was then adjusted to eliminate this drift. Span gas with a mixing ratio of 384.9 ppmv was then introduced into the hood and measured as 385.5 ppmv. This represents a gain drift of less than 0.2%. A similar procedure was applied to the H_2O channel using dry N_2 and a Licor LI-610 dew point generator. The offset was –3.2 mmole/mole and a dew point of 20.00 °C was measured as 19.65 °C. As a check of the CO_2 calibration, N_2 and a span gas (338.5 ppmv) were run in the field on DOY 201. The measured offset was –5.5 ppmv and the span gas was measured at 335.5 ppmv. This procedure was used for the second deployment with similar results.

FIELD MEASUREMENTS

To validate the system it was deployed to a pair of established AmeriFlux field sites on two different occasions. The AmeriFlux sites were located in north central Oklahoma, near the towns of Ponca City and Shidler.

TALLGRASS PRAIRIE DEPLOYMENT

The first deployment near Shidler, OK was at a native tallgrass prairie and lasted from 16-July-2000 (DOY 198) until 22-July-2000 (DOY 204). At the time of this deployment, the slow response sub-system wasn't finish and only the fast response system was taken to the field. The portable tower was set up approximately 8 meters west of the existing AmeriFlux tower. The IRGA was mounted on the west end, and the anemometer on the east end of the cross bar at the top of the tower and were separated by about 30 cm on this east-west line. The sonic anemometer was located 405 cm above ground level and the LI-7500 IRGA was located 375 cm above ground. The height of the prairie vegetation was about 40 cm. The permanent eddy covariance flux system was comprised of a Gill-Solent model R3 research grade sonic anemometer and a LiCor LI-6262 closed path IRGA. The R3 sonic anemometer is mounted 440 cm above ground and the IRGA inlet cup was attached to the anemometer body, just below the active volume. The sample flow rate was maintained at about 8 standard liters per minute (SLM). The IRGA was housed in a small, modified refrigerator and kept at a constant temperature. This system recorded its data on a desk top computer housed in a small, air conditioned shed and used a version of the same data collection program as was used by the portable system. Raw data from both the permanent and the portable systems were run through our reprocessing program.

Because the portable slow response system was not available for this deployment, we used meteorological data collected by the permanent system for flux reprocessing. A diurnal plot of CO_2 fluxes as measured by both the permanent and portable systems is shown in Figure 1. To more clearly illustrate how the two flux systems compare, Figure 2, presents CO_2 flux values measured by the portable, open-path LI-7500 based system as a function of flux values measured by the permanent, closed path LI-6262 based system. Similar data for latent heat fluxes is also available. Figure 3 presents a diurnal plot of latent heat fluxes while figure 4 shows the comparison between the two systems.

Besides using different IRGAs, the two flux systems also used different anemometers. To compare this aspect of the systems, we examine the sensible heat flux H, since all data for this quantity are measured by the anemometer. Figure 5 shows the diurnal series of sensible heat fluxes measured by both systems. Figure 6 is a comparison between sensible heat fluxes from our portable system and the permanent system. In addition to the sensible heat flux, we also consider the transfer of vertical momentum or the covariance between the vertical and horizontal wind velocities. A comparison between the two systems is shown in Figure 7.

WHEAT FIELD DEPLOYMENT

The second deployment was in a freshly plowed, fallow wheat field near Ponca City, OK. The existing AmeriFlux site at this location was instrumented identically to the tall grass prairie site. This deployment lasted from Oct. 3, 2000 (DOY 277) until Oct. 7, 2000 (DOY 281). The portable fast response tower was again set up approximately 10 meters to the west of the permanent AmeriFlux tower. The portable sonic anemometer was mounted 420 cm above ground and the IRGA was installed at 390 cm. Like the first deployment, they were separated by 30 cm on an east-west line. The slow response tower was located about half way between the portable fast response tower and the AmeriFlux tower. The cup anemometer and wind vane were 345 cm above ground and temperature/relative humidity sensors were located at 315 cm, 230 cm, 90 cm, and 20 cm above ground. In analyzing the profile data, it was noted that gradients in temperature and relative humidity involving the 20 cm T/R.H. sensor were all significantly different than other gradient pairs. For this reason, all gradients involving this sensor were discarded. The radiometer was mounted on the outrigger tower at a height of 235 cm above ground. During the time of this deployment, the site was bare soil and had been under drought conditions for a number of weeks. The field had been freshly turned over about a week prior to our deployment. Because of the lack of vegetation and soil moisture, we anticipated very small CO_2 fluxes. Because of these conditions (freshly turned over, extremely dry and hard soil chunks), we decided that the soil heat flux and soil temperature sensors could not be properly installed and would not perform adequately. Also since there was no vegetation, the PAR sensor also wasn't deployed. Our reasoning was that these sensors would add nothing of value to the experiment. We expected relatively large sensible heat fluxes and small latent heat fluxes (i.e. large Bowen ratios). These are the most difficult conditions to accurately apply the Webb-Pearman-Leuning corrections

for precise flux measurements with an open path sensor. Because of this, our goal for this deployment was to establish the suitability of the open path IRGA for small flux measurements under extreme field conditions. Since the range of CO_2 flux values obtained from this deployment is very limited, a direct comparison plot does not yield any new information that is not contained in Figure 2. Figure 8 shows the diurnal series of raw and the fully corrected CO_2 fluxes obtained from the portable system. In Figure 9, we show the corrected CO_2 fluxes from both systems.

As noted above, we had the slow response sub-system deployed at this site, and we measured vertical temperature and relative humidity profiles as well as the four components of the radiation budget (incoming short wave, incoming long wave, reflected short wave, and reflective long wave), available from the Kipp and Zonen CNR-1 radiometer. Besides being necessary inputs for modeling, these parameters are useful for validation of the eddy covariance fluxes. From the profile data, we can calculate the Bowen ratio and compare this with the same quantity calculated from eddy covariance data. We present a diurnal plot of Bowen ratios calculated from both the slow and fast systems in Figure 10. To investigate energy balance, we present a plot of the sum of H and LE versus net radiation (Rn) in Figure 11.

DISCUSSION OF FIELD RESULTS

The data in Figure 1 show good qualitative agreement between the two flux systems. We note in the figure, that there are several periods where the flux values from the portable system appear to have excessive noise. Most notable is the period from evening, DOY 198 to early morning, DOY 199. During this period, strong thunderstorms moved across the region and produced rain events at the flux tower site. Since the closed path sensor doesn't seem to be affected as badly as the open path IRGA, we assume that the noise is due to rainwater on the LI-7500 window. This was not unexpected behavior for an open path IRGA. When the LI-7500 was first installed, it was mounted vertically. After the rain, we tilted it about 30° away from vertical to promote runoff. Other rain events were noted in the early morning of DOY 202, and during the night and early morning of DOY 202 and 203. A regression fit to the data in Figure 2 yields a slope of 1.01 ±0.02 and an intercept of –0.7 μmole/m^2/sec (R^2=0.94) with a flux error estimate of ± 1.2 μmole/m^2/sec. The data span a range of +24 (uptake) to -14 (respiration) μmole/m^2/sec. As shown in Figure 2, CO_2 fluxes measured by the two systems compare very well with each other. The near unity slope of the regression fit and the small zero intercept indicate that the CO_2 fluxes calculated with the two

systems are virtually identical. Careful examination of Figure 2 also reveals that there are no apparent non-linear differences between the two systems. We note that the quality control criteria for this data ($u > 2$ m/sec, and $\sigma_{\rho CO2} < 1.1 \mu mole/m^3$) are fairly simple and may include data where the strict conditions for good flux measurements were not met. We chose this approach to include as many data points as possible, using the assumption that since the two flux towers were located close to each other, the measured fluxes should be the same regardless of whether they are representative of the entire fetch or not. This appears to be the case as witnessed by Figure 2.

The latent heat fluxes (LE) are shown in Figures 3 and 4. The one to one comparison of LE shown in Figure 4, indicates that there is some difference between the two systems. We note that the slope is 0.98 ±0.02 and the intercept is 10.9 W/m^2 (R^2=0.94) with a flux error estimate of ± 15 W/m^2. While the intercept is not excessive, it is significantly larger than the intercept of the sensible heat (H) comparison (see below). The slope suggests that the closed path, LI-6262 based permanent system may be underestimating LE by several percent. We also note that at small values of LE, there is a distinct non-linearity in the data, and that for small LE's, the open path system may perform significantly better than the closed path analyzer. This is consistent with expectations about closed path IRGAs and their response to water vapor. Water vapor has one of the strongest dipole moments of all of the permanent atmospheric gases. This implies that it will adsorb (or stick) to almost any surface, including the walls of a sampling tube and even the walls of a closed path analyzer cell. This could obviously cause serious high frequency loss in the water vapor spectral density, resulting in underestimation of the fluxes.

The regression fit to the sensible heat flux (H) shown in Figure 6 yields a slope of 0.93 ±0.01 and an intercept of 2.9 W/m^2 (R^2= 0.98) with a flux error estimate of ± 7 W/m^2. As with the CO_2 fluxes and the LE fluxes, this indicates good agreement between the two systems. The momentum flux of Figure 7 has a slope of 0.88 ±0.02 and an intercept of 14.6 gm-m/sec/sec with a flux error estimate of ± 11 gm-m/sec/sec. This is also acceptable agreement between two different instrument systems. The agreement in these two quantities suggests that both sonic anemometers behave similarly.

Examining figure 2 from Eugster et al (1997), we find that our CO_2 flux and LE flux slopes are considerably better than those obtained from their two flux systems at the same field site. The slope of our H flux, on the other hand was almost identical to theirs. Using the same arguments as Eugster, then, we

estimate that our system can resolve trend differences of 1% in CO_2 fluxes, 2% in LE fluxes, 7% in H fluxes, and 12% in momentum transfer fluxes when compared to similar permanent flux systems.

During the second deployment, we concentrated on measuring energy partitioning at the field site as well as making precise Webb-Pearman-Leuning corrections for CO_2 fluxes. As seen in Figure 8, the raw, uncorrected CO_2 flux (from the portable open path system) showed a very strong diurnal component. Because of the field conditions, we know that this apparent flux is not real. We know that there was no photosynthetic contribution to the fluxes and that, because of the extremely low soil moisture, the biogenic soil respiration component was also small. In fact, there should be very little diurnal pattern to the CO_2 fluxes observed. When the full Webb-Pearman-Leuning correction is applied, the resulting fluxes indeed loose all trace of a diurnal pattern. The corrected data shows that the flux was almost constant until DOY 279. In the early morning of DOY 279, the site received several millimeters of precipitation, which was absorbed by the surface soil. We see that the respirative CO_2 flux increases slightly, and then tapers off as the soil dries out again. This trend, while quite small is clearly seen in the corrected data. Figure 9 shows the fully corrected CO_2 fluxes from both the portable and permanent systems. The above-described behavior is evident in both systems and they agree quantitatively with each other quite well. The only significant difference between the two systems seems to be less variance in the portable fluxes as compared to the permanent system.

This was the first field deployment of the slow response subsystem. To add further confidence to the eddy covariance H and LE fluxes, we measured vertical profiles of temperature and relative humidity. From these slow response data, we calculated the Bowen ratio (β=H/LE). This was then compared with the Bowen ratio calculated from the fast response measurements of H and LE. As seen in Figure10, these two estimates of β agree fairly well. In the eddy covariance flux method, all measurements are made at the same height. In the gradient flux method, measurements are made at (at least) two distinct heights. This implies that gradient fluxes will not have as well defined fetches as those calculated from eddy covariance measurements. A rule of thumb is that the fetch from a gradient system will be approximately the same as an eddy covariance system mounted at a height equal to the geometric mean of the two gradient measurement heights. In our system, this difference of effective measuring heights is more than a meter, or

25% of the total eddy covariance height. The resulting fetch differences could easily account for the difference in Bowen ratios seen by the two systems.

Since the field conditions during this deployment were not conducive to soil parameter measurements, we cannot present a complete energy balance analysis. Instead, we show a plot of the total turbulent energy as measured by the eddy covariance system (H+LE) versus the net incoming solar radiation. Even without the soil heat flux and soil energy storage terms, we find fairly good agreement between these two quantities. The difference between the two could easily be due to the unmeasured soil heat flux and storage terms.

We note that even though these validation deployments were of limited duration, the data collected for the key eddy covariance fluxes (CO_2, LE, H) covered a large span of values. The comparison slopes for these quantities showed errors between 1% and 6.5%, indicating very little (if any) systematic differences between the two flux systems. The extremely small gain drifts observed during our calibrations verify that little field maintenance is required for the IRGA. While some small offset drifts were observed, these too are small and are eliminated in the eddy covariance process.

The actual deployment of the instruments went very smoothly. During the first deployment, the first two authors set up the fast response system in about 2 hours. During the second deployment, the first author set up both the fast and slow response towers alone in less than 4 hours. It should be noted, however, that these sites allowed easy and close vehicle access. For less accessible sites, longer set up times would be expected. All components of both subsystems fit easily for transportation in a minivan. All components easily break down into light sections, each less than 2 meters in length. The heaviest components are the batteries and the tripod towers, which weigh between 50 and 60 pounds each. The computer shelter unbolts into 6 flat panels if desired. After the second deployment, the entire system was dismantled, loaded, and ready to travel, in less than 2 hours. This meets our goals of portability and ease of set up.

CONCLUSIONS

As demonstrated by our validation deployments, the portable eddy covariance flux system described here meets all of our stated design goals. As shown by the short deployment times and minimal number of field personnel, the first two goals, portability and ease of setup are well met. The measured

power consumption of 35 watts is much less than the 150-200 watts previous systems based on closed path analyzers (Eugster et al., 1997). The majority of the power savings come from the elimination of the vacuum pump necessary in a closed path flux system. The excellent calibration stability and good comparison with the established AmeriFlux system show that we can expect a low maintenance and high accuracy flux system. Additionally, the close agreement with AmeriFlux closed path systems demonstrates that our portable system is capable of providing all the information needed to calculate accurate Webb-Pearman-Leuning corrections. The system performed well in all field conditions except during periods of moderate to heavy rain. While this is not desirable, we do not see it as a major liability. Finally, by using off-the-shelf parts and eliminating some instrument redundancies, this system can be built for a relatively low cost.

ACKNOWLEDGMENTS

The authors would like to express their gratitude to Prof. Shashi Verma of the University of Nebraska for allowing access to his research sites and for graciously sharing his data with us. We also wish to thank Mr. Sheldon Sharp of the University of Nebraska for his help in building several of the system components and Mr. John Martin of Ponca City, Oklahoma for his assistance at the filed sites.

This work was supported by the Atmospheric Radiation Measurement program (ARM), Office of Science, U.S. Department of Energy (DOE) under contract no. DE-AC03-76SF00098

REFERENCES

ARM SGP web site http://www.arm.gov/docs/sites/sgp/sgp.html

Chahuneau, F., Desjardins, R.L, Branch E., and Verdon, R., 1989. A Micrometeorological Facility for Eddy Flux Measurements of CO_2 and H_2O. J. Atmos. Oceanic Technol. 6, 193-200

Eugster, W., McFadden, J.P., Chapin, F.S., 1997. A Comparative Approach to Regional Variation in surface Fluxes Using Mobile Eddy Correlation Towers. Boundary-Layer Meteorol. 85, 293-307

Evans,R. AmeriFlux web site http://www.cdiac.esd.ornl.gov/programs/ameriflux/roving-system/roving_update_12-26-2000.htm and personal communication, 2000

Kaimal, J.C., Finnigan, J.J., 1994 Atmospheric Boundary Layer Flows: Their Structure and Measurement. Oxford University Press, New York

Kristensen, L., Mann, J., Oncley, S.P., Wyngaard, J.C., 1997. How close is close enough when measuring scalar fluxes with displaced sensors. J. Atmos. Oceanic Technol. 14, 814-821

Lee, X., 1998. On Micrometeorological Observations of Surface-Air Exchange Over Tall Vegetation. Agric. For. Meteorol. 91, 39-50

Moore, C.J., 1986. Frequency Response Corrections for Eddy Correlation Systems. Boundary-Layer Meteorol. 37, 17-35

Paw U, K.T., Baldocchi, D.D., Meyers, T.P., Wilson, K.B., Correction of Eddy-Covariance Measurements Incorporating Both Advective Effects and Density Fluxes. Boundary-Layer Meteorol. 97,487-511

Rannik, U. and Vesala, T., 1999. Autoregressive Filtering Versus Linear Detrending in Estimation of Fluxes by the Eddy Covariance Method. Boundary-Layer Meteorol. 91, 259-280

Schotanus, P., Nieuwstadt, F.T.M., and De Bruin, H.A.R., 1983. Temperature Measurement With a Sonic Anemometer and its Application to Heat and Moisture Fluxes. Boundary-Layer Meteorol. 26, 81-93

Sellers, P.J., Randall, A.D., Collatz, C.J., Berry, J.A., Field, C.B., Dazlich, D.A., Zhang, C., and Colello, G.D., 1996. A Revised Surface Parameterization (SiB2) for Atmospheric GCMs. Part 1: Model Formulation. J. Climate 9, 676-705

Webb, E.K., Pearman, G.I., and Leuning, R., 1980. Correction of Flux Measurements for Density Effects due to Heat and Water Vapour Transfer. Quart. J. Roy. Meteorol. Soc. 106, 85-100

Table 1.

INSTRUMENT	**FUNCTION**
Climatronics CS800-12 wind set	Mean horizontal wind speed and direction
Vaisala Humiter 50Y	Temperature and relative humidity profiles
Vaisala PTB101B barometer	Mean atmospheric pressure
HFT3 soil heat flux plates	Soil heat flux
TCAV soil thermocouple probe	Soil heat storage
LI-190SA quantum sensor	PAR
Kipp & Zonen CNR-1 radiometer	4-component radiometer (incoming and reflected in 2 bands, 0.3 μm – 2.8 μm and 5 μm – 50 μm)
TE525 tipping bucket rain gage	Mean precipitation

FIGURE CAPTIONS

Figure 1. Diurnal plot of the CO_2 fluxes measured during the first deployment (DOY 198 to DOY 204). The solid line are fluxes from the portable system and the dotted line are fluxes from the permanent system.

Figure 2. Comparison of quality controlled CO_2 fluxes between the portable system (horizontal axis) and the permanent system (vertical axis).

Figure 3. Diurnal plot of the latent heat (LE) fluxes measured during the first deployment (DOY 198 to DOY 204). The solid line are fluxes from the portable system and the dotted line are fluxes from the permanent system.

Figure 4. Comparison of LE fluxes between the portable system (horizontal axis) and the permanent system (vertical axis).

Figure 5. Diurnal plot of the sensible heat (H) fluxes measured during the first deployment (DOY 198 to DOY 204). The solid line are fluxes from the portable system and the dotted line are fluxes from the permanent system.

Figure 6. Comparison of H fluxes between the portable system (horizontal axis) and the permanent system (vertical axis).

Figure 7. Comparison of momentum transfer fluxes between the portable system (horizontal axis) and the permanent system (vertical axis).

Figure 8. Diurnal plot of the corrected (solid line) and uncorrected (dotted line) CO_2 fluxes obtained from the portable system during the second deployment (DOY 277 to DOY 281)

Figure 9. Diurnal plot of the corrected portable system (solid line) and corrected permanent system (dotted line) CO_2 fluxes obtained during the second deployment (DOY 277 to DOY 281)

Figure 10. Diurnal plot of the Bowen ratios (β) obtained from the portable system during the second deployment (DOY 277 to DOY 281). The solid line are data from the fast response eddy covariance sub-system and the dotted line are data from the slow-response profile sub-system.

Figure 11. Partial energy balance plot from data obtained during the second deployment (DOY 277 to DOY 281). The horizontal axis is net incoming radiation (Rn) obtained from the slow response sub-system, and the vertical axis is the sum of H and LE obtained from the fast response sub-system.

TABLE CAPTIONS

Table 1. Instrumentation and measurements made by the slow response system.

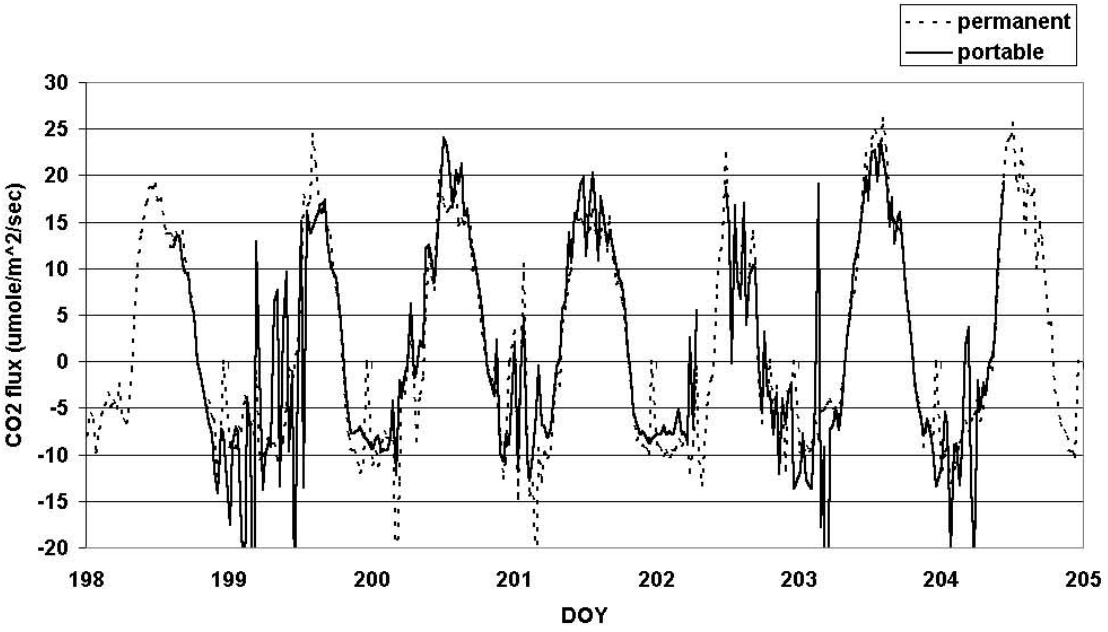
permanent
portable
CO2 flux (umole/m^2/sec)
30
25
20
15
10
5
0
-5
-10
-15
-20
198
199
200
201
202
203
204
205
DOY

Fig. 1

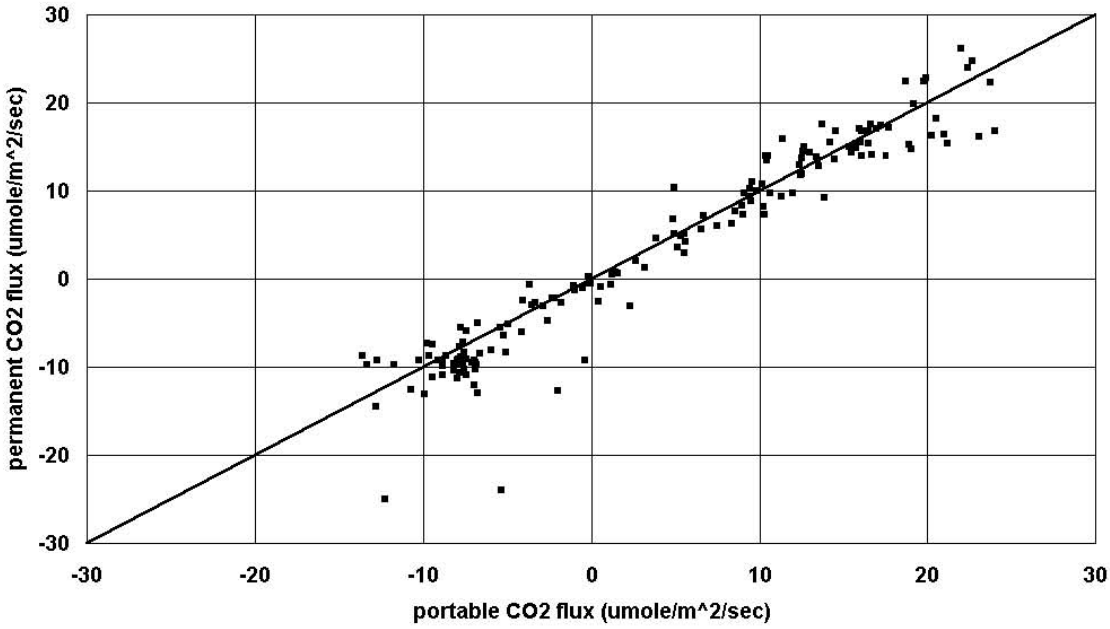
permanent CO2 flux (umole/m^2/sec)
30
20
10
0
-10
-20
-30
-30
-20
-10
0
10
20
30
portable CO2 flux (umole/m^2/sec)

Fig. 2

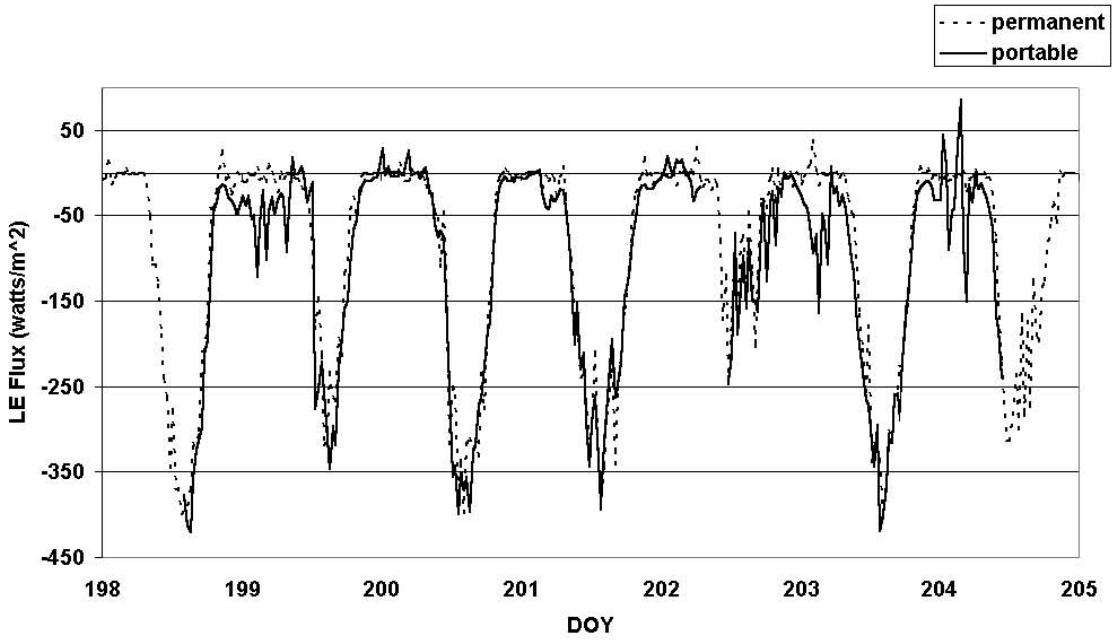
permanent
portable
LE Flux (watts/m^2)
50
-50
-150
-250
-350
-450
198
199
200
201
202
203
204
205
DOY

Fig. 3

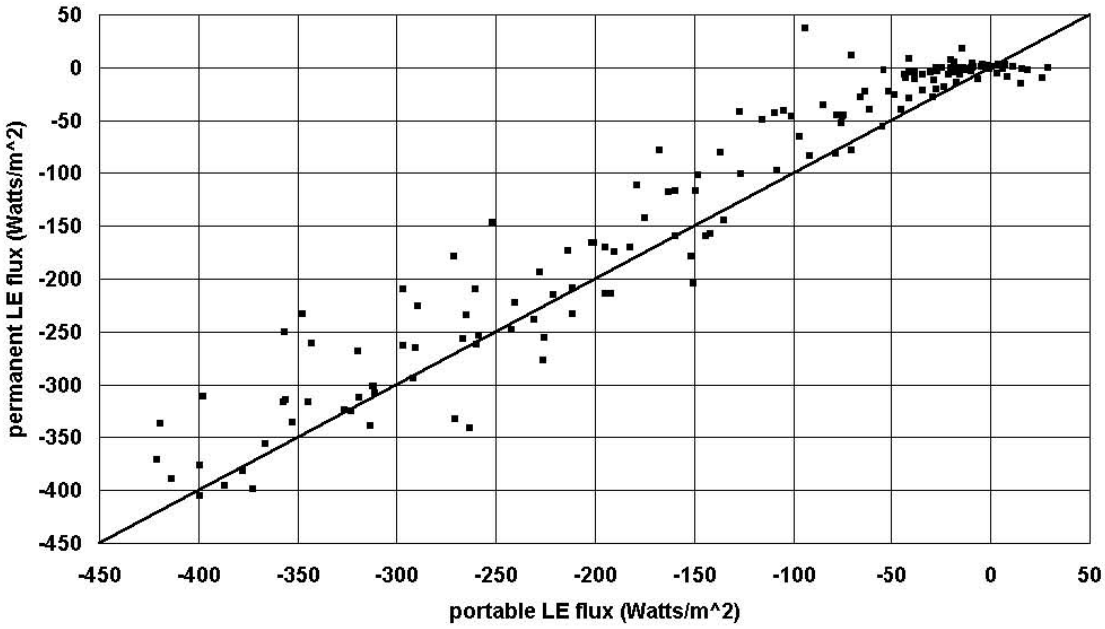
permanent LE flux (Watts/m^2)
50
0
-50
-100
-150
-200
-250
-300
-350
-400
-450
-450
-400
-350
-300
-250
-200
-150
-100
-50
0
50
portable LE flux (Watts/m^2)

Fig. 4

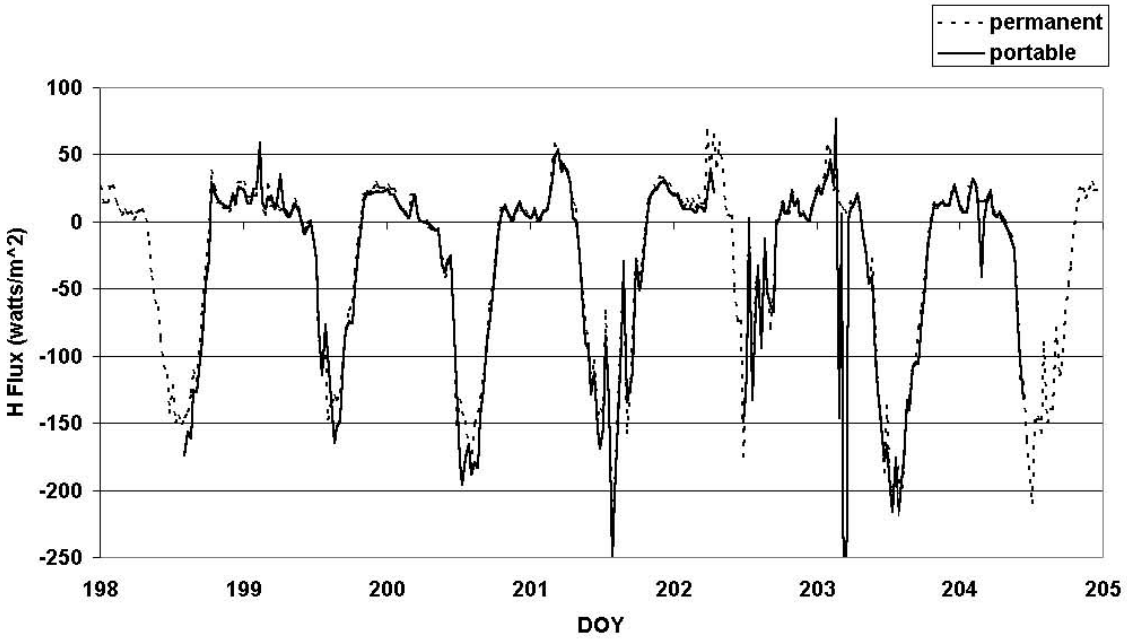
permanent
portable
100
50
0
-50
-100
-150
-200
-250
H Flux (watts/m^2)
198
199
200
201
202
203
204
205
DOY

Fig. 5

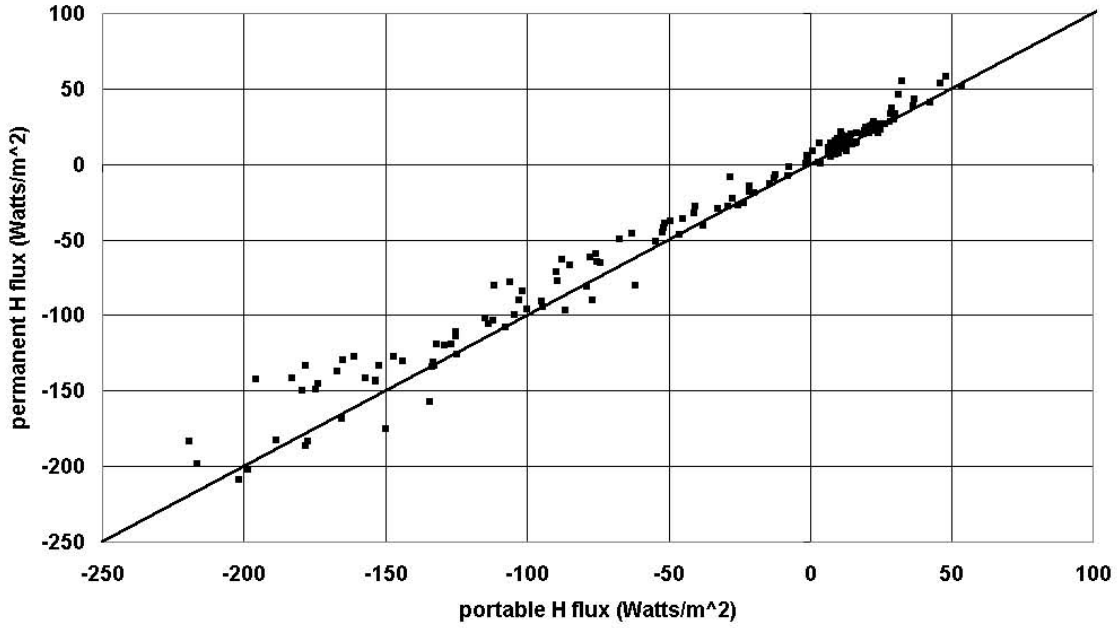
100
50
0
-50
-100
-150
-200
-250
permanent H flux (Watts/m^2)
-250
-200
-150
-100
-50
0
50
100
portable H flux (Watts/m^2)

Fig. 6

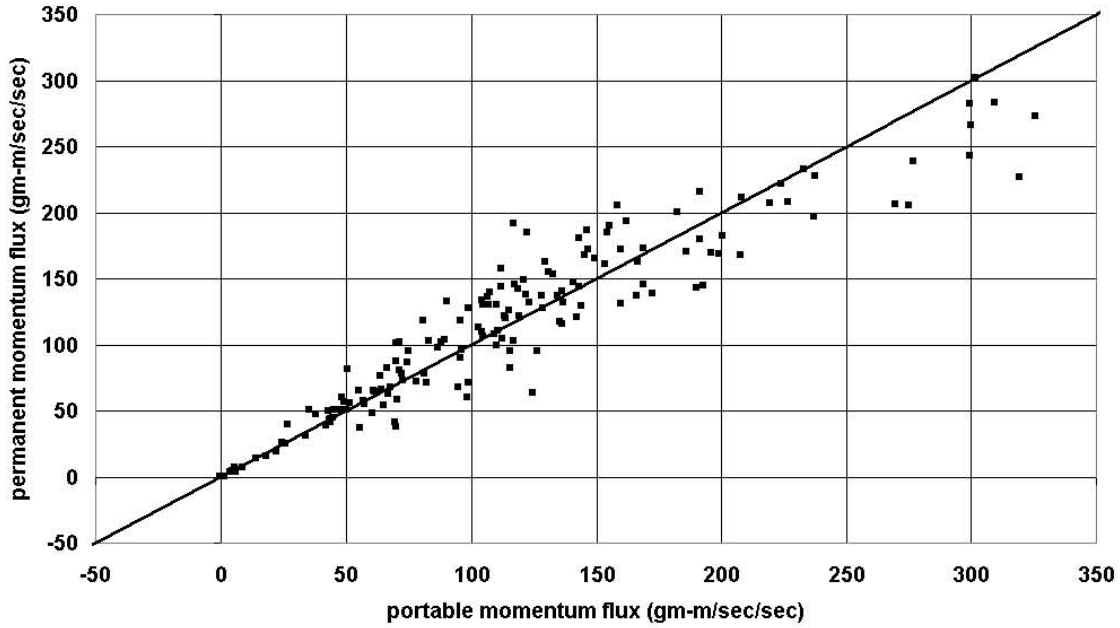
permanent momentum flux (gm-m/sec/sec)
portable momentum flux (gm-m/sec/sec)
350
300
250
200
150
100
50
0
-50
-50
0
50
100
150
200
250
300
350

Fig. 7

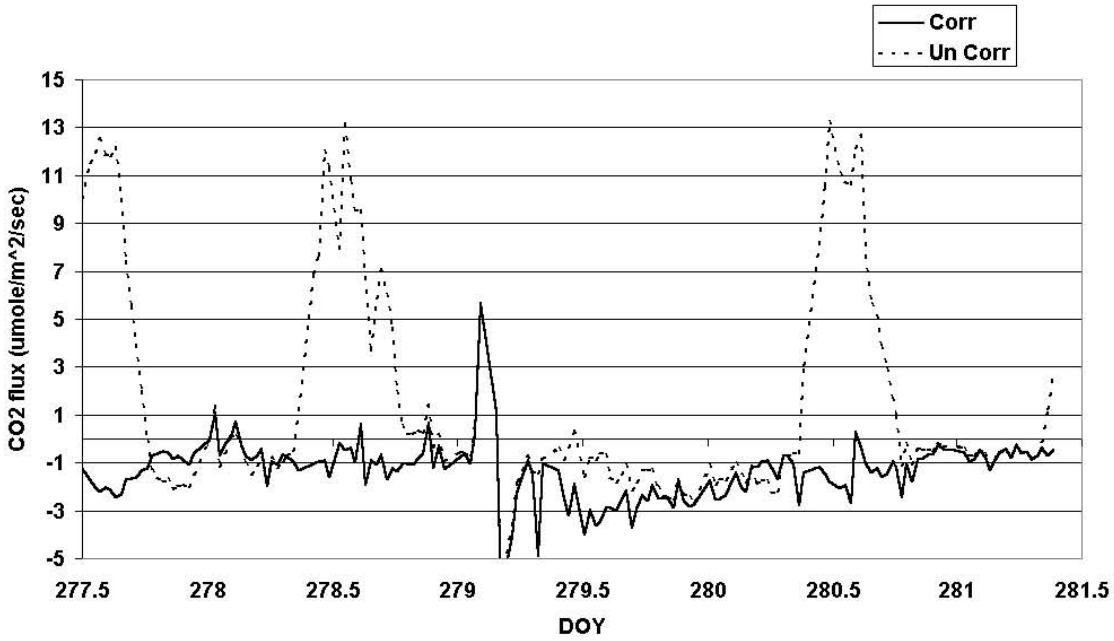
Corr
Un Corr
CO2 flux (umole/m^2/sec)
DOY
15
13
11
9
7
5
3
1
-1
-3
-5
277.5
278
278.5
279
279.5
280
280.5
281
281.5

Fig. 8

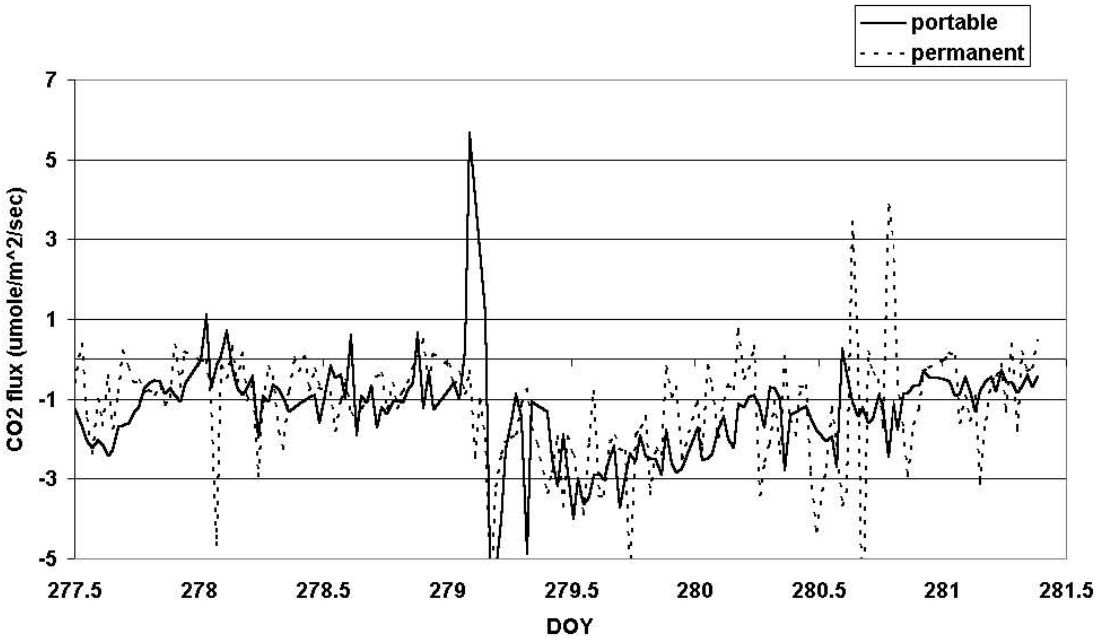
portable
permanent
CO2 flux (umole/m^2/sec)
7
5
3
1
-1
-3
-5
277.5
278
278.5
279
279.5
280
280.5
281
281.5
DOY

Fig. 9

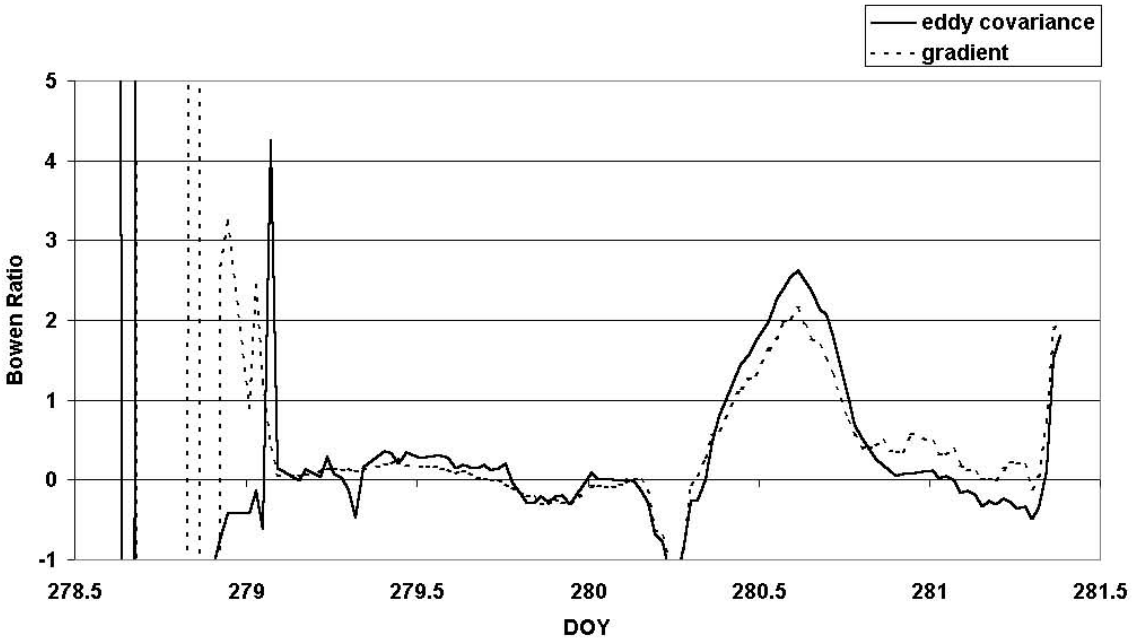
eddy covariance
gradient
Bowen Ratio
5
4
3
2
1
0
-1
278.5
279
279.5
280
280.5
281
281.5
DOY

Fig. 10

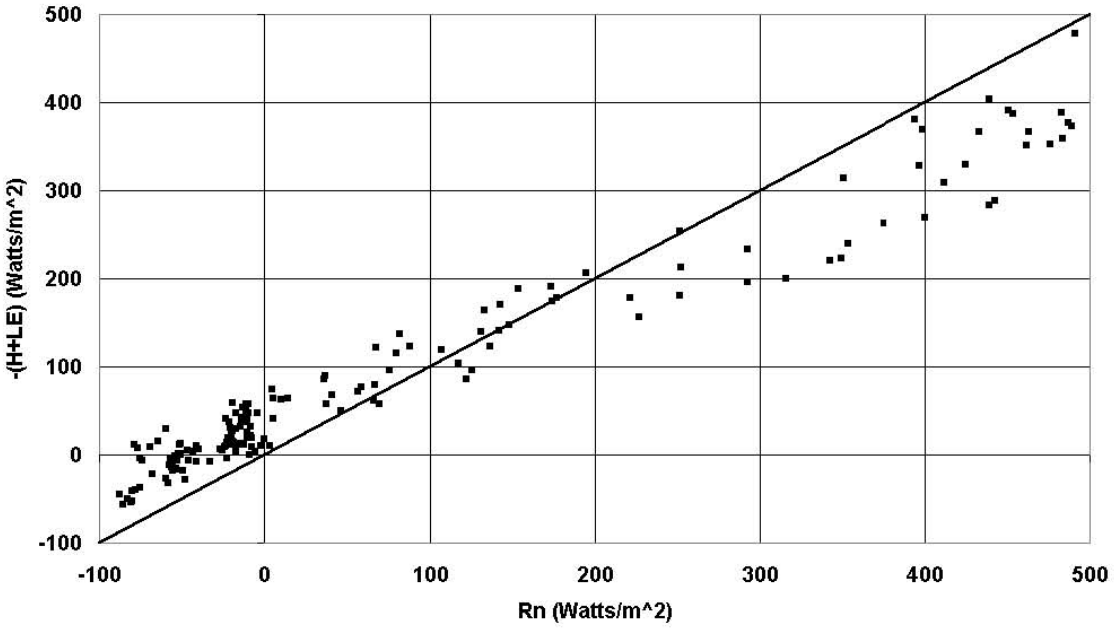
500
400
300
200
100
0
-100
-(H+LE) (Watts/m^2)
-100
0
100
200
300
400
500
Rn (Watts/m^2)

Fig. 11